Anisotropic *s*-wave superconductivity in CaAlSi single crystals from penetration depth measurements

Ruslan Prozorov
Ames Laboratory and Department of Physics and Astronomy, Iowa State University, Ames, Iowa 50011, USA

Tyson A. Olheiser and Russell W. Giannetta
Department of Physics, University of Illinois at Urbana-Champaign, 1110 West Green Street, Urbana, Illinois 61801, USA

Kentaro Uozato and Tsuyoshi Tamegai
Department of Applied Physics, The University of Tokyo, Hongo, Bunkyo-ku, Tokyo 113-8656, Japan
(Received 28 February 2006; published 23 May 2006)

In- and out-of-plane London penetration depths were measured in CaAlSi single crystals (T_c=6.2 and 7.3 K) using a tunnel-diode resonator. A full three-dimensional (3D) BCS analysis of the superfluid density is consistent with a prolate spheroidal gap, with a weak-coupling BCS value in the *ab* plane and stronger coupling along the *c* axis. The gap anisotropy was found to significantly decrease for higher T_c samples.

DOI: 10.1103/PhysRevB.73.184523 PACS number(s): 74.25.Nf, 74.20.Rp, 74.70.Ad

Superconductors with an AlB_2 structure have received increased attention after the discovery of superconductivity at 39 K and especially after identification of two distinct gaps in MgB_2.[1–3] It is believed that two gaps survive because of reduced interband scattering due to the different dimensionality of two-dimensional (2D) σ and three-dimensional (3D) π bands. Investigating materials with similar crystal and band structure is therefore important for understanding the mechanism of superconductivity in this class of hexagonal-layer compounds. In this paper we study CaAlSi which has been synthesized long ago,[4] but in which superconductivity was discovered only recently.[5] Band structure calculations show highly hybridized three-dimensional interlayer and π^* bands.[6,7] Although most studies of CaAlSi indicate *s*-wave pairing, deviations from a single isotropic gap behavior have been reported.[5,8–11] Magnetic measurements indicate a fully developed *s*-wave BCS gap.[9,12] Angle-resolved photoemission spectroscopy[10] revealed the same gap magnitude on the two bands with a moderately strong coupling value for the reduced gap $2\Delta/k_BT_c$=4.2. Together with specific heat measurements[11] it provided reliable evidence for a three-dimensional moderately strong-coupled *s*-wave BCS superconductivity. On the other hand, μSR studies have been interpreted as evidence of either one highly anisotropic or two distinct energy gaps.[8] Furthermore, five-fold and six-fold stacking sequences of (Al,Si) layers corresponding to two different values of T_c of ~6 and ~8 K were found.[13] Therefore, an experimental study of in- and out-of-plane superfluid density is needed to understand the anisotropic superconducting gap structure and to elucidate the mechanism of superconductivity in AlB_2 type compounds.

Single crystals of CaAlSi were grown from Ca:Al:Si (1:1:1) ignots using a floating zone method as described elsewhere.[18] Samples have T_c either 6.2 or 7.3 K, which is directly related to different stacking sequences.[13] We measured two of each type of slab-shaped crystals with typical dimensions $0.3\times0.3\times0.4$ mm^3. The penetration depth was measured with an *LC* tunnel-diode oscillator which is sensitive to changes in the susceptibility of several pico-emu or, equivalently, to changes in the London penetration depth of about 0.3 Å for our crystals.[16] The quantitative analysis of the frequency shift depends on the sample shape and relative orientation of the excitation field H_{ac} with respect to the principal axes. Assuming a superconducting crystal with an isotropic in-plane response determined by the in-plane penetration depth $\lambda_{ab}(T)$ and possibly different *c*-axis penetration depth $\lambda_c(T)$ at least two experimental arrangements are required to extract $\lambda_{ab}(T)$ and $\lambda_c(T)$ separately. In the $H_{ac}\|c$-axis orientation, superconducting currents are generated in the *ab* plane, thus the susceptibility is determined only by $\lambda_{ab}(T)$ and the frequency shift $\Delta f(T)=f(T)-f_0$ is given by

$$\Delta f(T) = \frac{f_0 V_s}{2V_0(1-N)}\left[1-\frac{\lambda(T)}{R}\tanh\left(\frac{R}{\lambda(T)}\right)\right], \qquad (1)$$

where V_0 is the effective coil volume, N is the demagnetization factor, $\lambda(T)$ is the London penetration depth, and R is the effective planar sample dimension.[16] With magnetic susceptibility χ this equation is just $\Delta f(T)=-4\pi\chi(T)\Delta f_0$ where the only sample shape-dependent parameter Δf_0 is measured directly by pulling the sample out of the coil at a low temperature.

Figure 1 shows the in-plane penetration depth determined from the frequency shift using Eq. (1). The zero-temperature value was estimated from the fit to the BCS formula as described below. This value is not important for the analysis of $\Delta\lambda_{ab}(T)$, but is needed to estimate the superfluid density. Muon spin rotation gives $\lambda_{ab}(0)$=2390 Å,[8] measurements of the critical field $\lambda_{ab}(0)$=3140 Å,[9] and reversible magnetization $\lambda_{ab}(0)$=3100 Å.[9] Our conclusions are not significantly affected by the variation of these values. The main purpose of Fig. 1 is to compare crystals with different T_c. The inset shows data on a full temperature scale. The signal saturates at the level corresponding to the normal-state skin depth, thus providing additional information—contactless measurements of the resistivity above the transition. We find 45 and 33 $\mu\Omega$ cm for T_c=6.2 and 7.3 K, respectively, which is in an

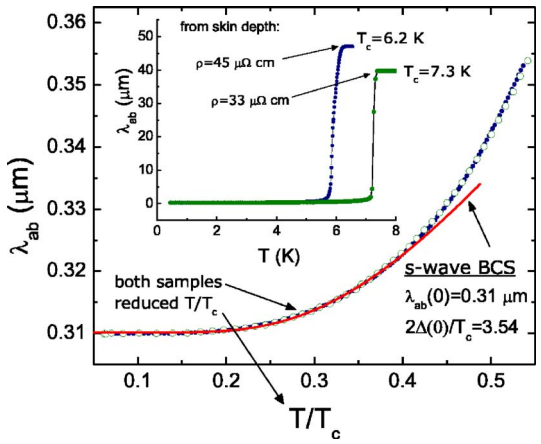

FIG. 1. (Color online) Low-temperature variation of the in-plane penetration depth in two crystals plotted versus reduced temperature T/T_c. The Red line is a fit to a low-temperature *s*-wave BCS model, Eq. (2). The inset shows a full temperature scale along with the normal state resistivities extracted from the skin depth.

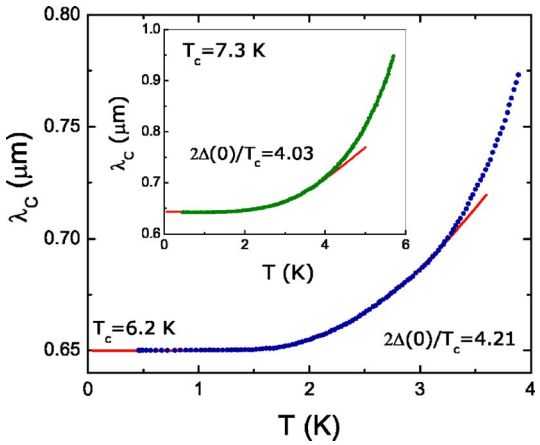

FIG. 2. (Color online) *c*-axis penetration depth obtained from the numerical inversion of Eq. (3) for two different samples. Main frame—for sample with $T_c=6.2$ K and the inset shows a sample with $T_c=7.3$ K. Solid lines are fits to the low-temperature BCS expression, Eq. (2).

agreement with direct measurements on single crystals, which found 36 $\mu\Omega$ cm on a higher T_c sample.[17,18] On the contrary, when $\lambda_{ab}(T)$ is plotted versus a reduced temperature T/T_c, the curves for the two samples coincide (no normalization was done for the *y* axis). The open symbols in Fig. 1 show the results for $T_c=7.3$ K crystal, whereas closed symbols show $T_c=6.2$ K material. The data are well fit by the standard weak-coupling *s*-wave BCS model

$$\frac{\Delta\lambda(T)}{\lambda(0)} = \sqrt{\frac{\pi\Delta(0)}{2T}}\exp\left(-\frac{\Delta(0)}{T}\right), \tag{2}$$

where, from $\Delta\lambda_{ab}(T)$, we obtained $\Delta_{ab}(0)=1.76k_BT_c$–a weak-coupling *s*-wave BCS superconducting gap.

In the $H_{ac}\|ab$ orientation shielding currents flow along both the *ab* plane and the *c* axis. The full magnetic susceptibility is obtained from the anisotropic London equation, which must be solved numerically to extract the interplane penetration depth $\lambda_c(T)$. For a slab $2b\times 2d\times 2w$ with magnetic field oriented along the longest side *w* the following solution has been obtained:[19]

$$\frac{\Delta f_c(T)}{\Delta f_0^{H\|ab}} = 1 - \frac{\lambda_{ab}}{d}\tanh\left(\frac{d}{\lambda_{ab}}\right) - 2\lambda_c b^2\sum_{n=0}^{\infty}\frac{\tanh(\tilde{b}_n/\lambda_c)}{k_n^2\tilde{b}_n^3}, \tag{3}$$

where $k_n=\pi(n+1/2)$ and $\tilde{b}_n=b\sqrt{[(k_n\lambda_{ab}/d)^2+1]}$. Knowing $\lambda_{ab}(T)$ from independent measurements in the $H_{ac}\|c$ orientation and measuring the total frequency shift upon extraction of the sample from the coil $\Delta f_0^{H\|ab}$, Eq. (3) is solved numerically to obtain $\lambda_c(T)$.

Figure 2 shows the out-of-plane penetration depth obtained from Eq. (3). The main frame shows the $T_c=6.2$ K sample, whereas the inset shows data for the $T_c=7.3$ K sample. The solid lines are the fits to the low-temperature isotropic BCS expression, Eq. (2). The gap amplitude obtained from the fits indicates stronger coupling along the *c* axis [compared to the $\lambda_{ab}(T)$ fits, Fig. 1]. However, as shown below, such fitting significantly underestimates the anisotropy of the superconducting gap. The major problem is that Eq. (2) is only valid for an isotropic gap that is constant with temperature, restricting its range of validity to $T/T_c<0.35$. This restriction excludes a significant portion of the data. A more comprehensive analysis requires a determination of the normalized superfluid density, which is obtained from the measured change in the penetration depth $\Delta\lambda(T)$ via $\rho(T)=[1+\Delta\lambda(T)/\lambda(0)]^{-2}$.

The superfluid density generally depends on the shape of the Fermi surface and the gap anisotropy.[20] For CaAlSi we can assume a fairly isotropic Fermi surface,[6,7,21] a superconducting gap isotropic in the *ab* plane, and anisotropic for the out-of-plane response. Within the semiclassical approximation,[20]

$$\rho_{ab} = 1 - \frac{3}{4T}\int_0^1 (1-z^2)\left[\int_0^\infty \cosh^{-2}\left(\frac{\sqrt{\varepsilon^2+\Delta(z)^2}}{2T}\right)d\varepsilon\right]dz, \tag{4}$$

$$\rho_c = 1 - \frac{3}{2T}\int_0^1 z^2\left[\int_0^\infty \cosh^{-2}\left(\frac{\sqrt{\varepsilon^2+\Delta(z)^2}}{2T}\right)d\varepsilon\right]dz, \tag{5}$$

where $z=\cos(\theta)$ and θ is the polar angle with $\theta=0$ along the *c* axis. Since there is no general argument for the shape of the gap, we choose the spheroidal form

$$\Delta(T,\theta) = \frac{\Delta_{ab}(T)}{\sqrt{1-\varepsilon\cos^2(\theta)}} \tag{6}$$

and parameter $-\infty\leq\varepsilon\leq 1$ is related to eccentricity *e* as $\varepsilon=e^2=1-c^{-1}$ where *c* is the normalized semiaxis along the *c* axis, but ε can assume both negative and positive values. The spheroid is either prolate ($\varepsilon>0$), oblate ($\varepsilon<0$), or a sphere ($\varepsilon=0$). The temperature dependence of the superconducting gap was obtained from the anisotropic gap equation. We found that it is well approximated by $\Delta(T)=\Delta(0)\tanh(1.785\sqrt{T_c/T-1})$.

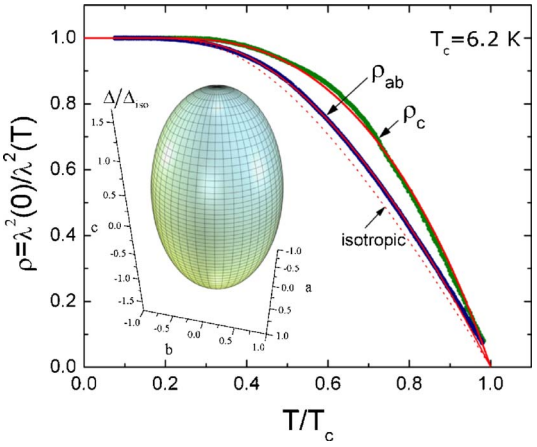

FIG. 3. (Color online) Two components of the superfluid density for samples with $T_c=6.2$ K. Symbols show measured data and solid lines show corresponding full 3D fiiting. The dashed line shows an isotropic *s*-wave BCS result. The inset shows an ellipsoidal gap that describes both curves.

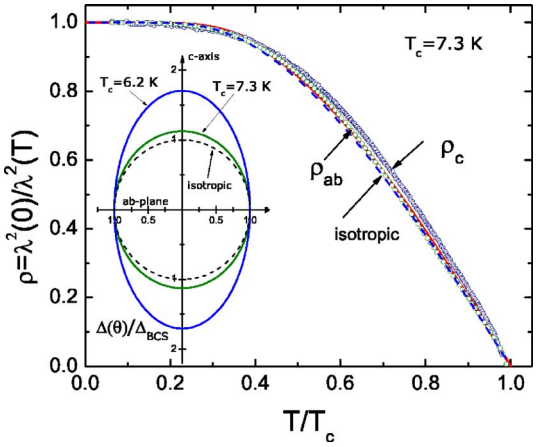

FIG. 4. (Color online) Superfluid densities for the higher $T_c=7.3$ K samples showing an apparent reduction of the gap anisotropy compared to Fig. 3. The inset compares a cross section of the gap amplitude for the two cases.

The following data analysis was performed. By measuring the same sample in two orthogonal orientations (along the *c* axis and along the *ab* plane), both $\lambda_{ab}(T)$ and Δf_c were obtained. The latter contains contributions from both $\lambda_{ab}(T)$ and $\lambda_c(T)$. Equation (3) was then used to numerically evaluate $\lambda_c(T)$. Low-temperature BCS fits as well as measurements of the reversible magnetization were used to estimate $\lambda_{ab}(0)=0.31$ μm and $\lambda_c(0)=0.65$ μm. Fits over the full temperature range confirmed the assumed values. Then Eqs. (4) and (5) were used to fit the data. As a final step, both curves $\rho_{ab}(T)$ and $\rho_c(T)$ were generated from a single set of fitting parameters.

Figure 3 shows data and fitting results for the lower $T_c=6.2$ K samples. Symbols are the measured data points and solid lines are calculated for the ellipsoidal gap shown in the inset. The fitting procedure yielded the weak-coupling BCS value $2\Delta_{ab}(0)/k_BT_c=3.53$ in the *ab* plane and $\varepsilon=0.656$ corresponding to $2\Delta_c(0)/k_BT_c=6.02$ gap maximum along the *c* axis.

Figure 4 shows similar results for the samples with $T_c=7.3$ K. There is an obvious reduction of the gap anisotropy. The best fit to the ellipsoidal gap yields $\varepsilon=0.206$ resulting in $2\Delta_c(0)/k_BT_c=3.98$. It should be noted that in most previous works only averaged values of the superconducting gap could be obtained. From heat capacity measurements, $2\Delta(0)/k_BT_c=4.07$ was obtained,[11] whereas ARPES yielded $2\Delta(0)/k_BT_c=4.2$.[10] The average effective gap can be obtained from our results by equating volumes of the spheroidal gap and a sphere, $\Delta_{eff}=\Delta_{ab}(0)(1-\varepsilon)^{-1/6}$. This gives $2\Delta_{eff}(0)/k_BT_c=4.22$ for samples with $T_c=6.2$ K and $2\Delta_{eff}(0)/k_BT_c=3.66$ for samples with $T_c=7.3$ K which is in the correct range of reported values and our earlier fits using Eq. (2). All these values should be compared to the weak-coupling isotropic result of $2\Delta(0)/k_BT_c=3.53$.

For all samples studied, we find that the temperature dependencies of both in-plane and out-of-plane superfluid density are fully consistent with single-gap anisotropic *s*-wave superconductivity. The gap magnitude in the *ab* plane is close to the weak-coupling BCS value while the *c* axis values are somewhat larger. Our results suggest that scattering is not responsible for the difference in T_c. Scattering would lead to a suppression of the gap anisotropy.[22] The gap with average value $\bar{\Delta}$ and variation $\delta\Delta$ on the Fermi surface can only survive if $\hbar\tau^{-1}\ll\sqrt{\bar{\Delta}\delta\Delta}$, where τ is the impurity scattering rate.[22] The values of resistivity are very close for both high- and low-T_c samples (45 and 33 $\mu\Omega$ cm, respectively); see Fig. 1, the qualitative trend in anisotropy is just opposite. Also, 15% suppression of T_c by nonmagentic impurities requires very large concentrations. This would, indeed, significantly smear the transition, which we did not observe. Therefore, all facts point out that in a CaAlSi gap anisotropy abruptly decreases as T_c abruptly increases from $\sim$6 to $\sim$8 K. A plausible mechanism comes from the analysis of the stacking sequence of (Al/Si) hexagonal layers.[13] There are two structures—five-fold and six-fold stacking corresponding to low- and higher-T_c samples, respectively. The buckling of (Al,Si) layers is greatly reduced in a six-fold structure, which leads to the enhancement of the density of states, hence higher T_c. Our results suggest that reduced buckling also leads to almost isotropic gap function. This may be due to significant changes in the phonon spectrum and anisotropy of the electron-phonon coupling.

Measurements of the field dependence of the penetration depth in the vortex state also show a difference between the two sets of samples, as do measurements taken with different field orientations relative to the *c* axis. Of particular interest is the variation of the second critical field and the so-called peak effect.[9,14,15,17,18] Tunnel-diode studies of these properties will be reported elsewhere.

We would like to thank Vladimir Kogan and Jules Carbotte for helpful discussions related to the connection between measured London penetration depth, anisotropy, strong coupling, and two-band superconductivity. Ames Laboratory is operated for the U.S. Department of Energy by Iowa State University under Contract No. W-7405-ENG-82.

This work was supported in part by the Director for Energy Research, Office of Basic Energy Sciences and in part by NSF Grant No. DMR-0603841. R.P. acknowledges support from the Alfred P. Sloan Foundation. R.W.G. and T.A.O. acknowledge support from the National Science Foundation, Contract No. DMR 05-03882. K.U. and T.T. acknowledge support by a Grant-in-aid from the Ministry of Education, Culture, Sports, Science, and Technology.

[1] T. Muranaka, Y. Zenitani, J. Shimoyama, and J. Akimitsu, Frontiers in Superconducting Materials, 937 (2005).
[2] P. C. Canfield, and S. Bud'ko, Sci. Am. **292**, 80 (2005).
[3] F. Bouquet, Y. Wang, R. A. Fisher, D. G. Hinks, J. D. Jorgensen, A. Junod, and N. E. Phillips, Europhys. Lett. **56**, 856 (2001).
[4] O. I. Bodak, E. I. Gladyshevskii, O. S. Zarechnyuk, and E. E. Cherkashin, Visn. L'viv. Gos. Univ. Ser. Khim. **8**, 75 (1965).
[5] M. Imai, K. Nishida, T. Kimura, and H. Abe, Appl. Phys. Lett. **80**, 1019 (2002).
[6] I. I. Mazin and D. A. Papaconstantopoulos, Phys. Rev. B **69**, 180512(R) (2004).
[7] M. Giantomassi, L. Boeri, and G. B. Bachelet, Phys. Rev. B **72**, 224512 (2005).
[8] S. Kuroiwa, H. Takagiwa, M. Yamazawa, J. Akimitsu, K. Ohishi, A. Koda, W. Higemoto, and R. Kadono, J. Phys. Soc. Jpn. **73**, 2631 (2004).
[9] A. K. Ghosh, Y. Hiraoka, M. Tokunaga, and T. Tamegai, Phys. Rev. B **68**, 134503 (2003).
[10] S. Tsuda, T. Yokoya, S. Shin, M. Imai, and I. Hase, Phys. Rev. B **69**, 100506(R) (2004).
[11] B. Lorenz, J. Cmaidalka, R. L. Meng, and C. W. Chu, Phys. Rev. B **68**, 014512 (2003).
[12] M. Imai, El Hadi, S. Sadki, H. Abe, K. Nishida, T. Kimura, T. Sato, K. Hirata, and H. Kitazawa, Phys. Rev. B **68**, 064512 (2003).
[13] H. Sagayama, Y. Wakabayashi, H. Sawa, T. Kamiyama, A. Hoshikawa, S. Harjo, K. Uozato, A. K. Ghosh, M. Tokunaga, and T. Tamegai, J. Phys. Soc. Jpn. **75**, 043713 (2006).
[14] T. Tamegai, K. Uozato, A. K. Ghosh, and M. Tokunaga, Int. J. Mod. Phys. B **19**, 369 (2004).
[15] T. Tamegai, Z. Shi, A. K. Pradhan, H. Nakamura, A. K. Ghosh, M. Tokunaga, Y. Takano, K. Togano, H. Kito, and H. Ihara, J. Low Temp. Phys. **131**, 1153 (2003).
[16] R. Prozorov, R. W. Giannetta, A. Carrington, and F. M. Araujo-Moreira, Phys. Rev. B **62**, 115 (2000).
[17] A. K. Ghosh, Y. Hiraoka, M. Tokunaga, and T. Tamegai, Physica C **392–396**, 29 (2003).
[18] A. K. Ghosh, M. Tokunaga, and T. Tamegai, Phys. Rev. B **68**, 054507 (2003).
[19] P. A. Mansky, P. M. Chaikin, and R. C. Haddon, Phys. Rev. B **50**, 15929 (1994).
[20] B. S. Chandrasekhar and D. Einzel, Ann. Phys. **2**, 535 (1993).
[21] I. R. Shein, N. I. Medvedeva, and A. L. Ivanovskii, J. Phys.: Condens. Matter **15**, L541 (2003).
[22] I. I. Mazin, O. K. Andersen, O. Jepsen, A. A. Golubov, O. V. Dolgov, and J. Kortus, Phys. Rev. B **69**, 056501 (2004).